

Characterization of Radio Propagation Channel in Urban Vehicle to Infrastructure Environments to Support WSNs [†]

Fausto Granda ^{1,2}, Leyre Azpilicueta ^{2,*}, Cesar Vargas-Rosales ², Peio Lopez-Iturri ³, Erik Aguirre ³, José Javier Astrain ⁴, Jesus Villandangos ⁴ and Francisco Falcone ³

¹ Universidad de las Fuerzas Armadas ESPE, Sangolquí 171-5-231B, Ecuador; flgranda@espe.edu.ec

² School of Engineering and Sciences, Tecnológico de Monterrey, Monterrey 64849, Mexico; cvargas@itesm.mx

³ Electrical and Electronic Engineering Department, Public University of Navarre, Pamplona, Navarra 31006, Spain; peio.lopez@unavarra.es (P.L.-I.); erik.aguirre@unavarra.es (E.A.); francisco.falcone@unavarra.es (F.F.)

⁴ Mathematical Engineering and Computer Science Department, Public University of Navarre, Pamplona, Navarra 31006, Spain; josej.astrain@unavarra.es (J.J.A.); jesusv@unavarra.es (J.V.)

* Correspondence: leyre.azpilicueta@itesm.mx; Tel.: +52-81582082; Fax: +52-8183597211

[†] Presented at the 3rd International Electronic Conference on Sensors and Applications, 15–30 November 2016; Available online: <https://sciforum.net/conference/ecsa-3>.

Published: 14 November 2016

Abstract: Vehicular ad hoc Networks (VANETs) enable vehicles to communicate with each other as well as with roadside units (RSUs). Although there is a significant research effort in radio channel modelling focused in vehicle to vehicle (V2V), not much work has been done for vehicle to infrastructure (V2I) using 3D ray-tracing tools. This work evaluates some important parameters of a V2I wireless channel link such as Received Power, Power Delay Profile, Delay Spread and Coherence Bandwidth, in an urban scenario using a deterministic simulation model based on an in-house 3D Ray-Launching algorithm. Analysis using Wireless Sensor Networks (WSNs) at 868MHz, 2.4 and 5.9 GHz are presented. Results show the highly impact that the distance, link frequency, location of RSUs and obstacles in the LoS (Line of Sight) have in V2I channel propagation. These results constitute the start point in the deployment of radio-planning in V2I environments.

Keywords: Wireless Sensor Networks (WSN); 3D ray launching; vehicular ad-hoc Networks (VANET); vehicle-to-infrastructure communication (V2I)

1. Introduction

In 2014, a total of approximately 200,000 deaths were classified as injury related in United States, where motor-vehicle traffic-related injuries resulted in 33,736 deaths, accounting for 16.9% of all injury deaths [1]. In Japan, over 60% of traffic accident fatalities are the result of vehicle collisions with pedestrians/bicyclists and intersection collisions [2]. In Mexico during 2015, the traffic accidents in urban and suburban zones caused 111,000 victims were 4.1% resulted in death between drivers, passengers, pedestrians, cyclists and others [3]. The protection of drivers, passengers, pedestrians, bicyclists, motorcyclist and other vehicle and nonvehicle occupants is part of ongoing efforts in the world, in the area of Intelligent Transportation System (ITS) where connected vehicles research includes three major approaches to communication: Vehicle to Vehicle (V2V), Vehicle to Infrastructure (V2I) and Vehicle to Pedestrian (V2P). The V2I Communications is the bi-directional wireless exchange of data (control and information) between vehicles and Road Side Units (RSUs). In 1999, the U.S. Federal Communication Commission (FCC) allocated a 75 MHz spectrum at 5.9GHz to be used as V2V and V2I communications known as Dedicated Short Range Communications

(DSRC), and the IEEE 802.11p standard [4] was developed for operation at 5.9 GHz. In Europe the government have licensed the 5.9 GHz while in Japan have licensed the 5.8 GHz for vehicular communications.

In the V2I urban environment, a combination of different object types as buildings, vehicles (both static and mobile), and vegetation, as well as their number, size, and density, has a profound impact on the radio propagation [5]. Some propagation impairments are analogous at the presented in short-range outdoor radio communication systems [6]: reflection from, diffraction around and transmission loss through objects (influence of vegetation, building entry loss, cars, trees, pedestrians, etc.), external environment, which gives rise to issues such as temporal and spatial variation of path loss and multipath effects from reflected and diffracted components of the wave. Over the past 7 or 8 years, much research has been dedicated to V2V communication systems [7], and there exists a need for further studies to investigate V2I and V2P channels. Indeed, for the author’s knowledge, there are few scientific work for V2I propagation analysis, even less using deterministic tools for urban environments. In this work, a deterministic method has been used, specifically an in-house 3D Ray Launching (RL) algorithm, based on Geometrical Optics (GO) and Geometrical Theory of Diffraction (GTD). The detailed operating mode of the algorithm has been previously published [8], and validated in transportation systems [9].

The remaining parts of the paper are arranged as follow: characterization and scenery simulation are explained in Section 2. Section 3 presents the results of the analysis: Received Power (RP), Power delay Profile (PDP), Root-Mean-Square Delay Spread (RMS delay spread) and Coherence Bandwidth (CB), where the antenna transmitter (Tx) is located at RSU level and the antenna receiver (Rx) is located at vehicle level. Conclusions and future work are shown in Section 4.

2. Simulation Urban Scenario

Figure 1a show a 3D frontal-view that represents the scenario modeled and used for simulation and Figure 1b is a 2D back-view that displays the position reference level (x, y) and the identification of different areas of interest used later, according to Table 1.

The ray launching tool incorporate a database of geographic data such as vegetation, terrain, buildings, park-benches, cars, pedestrians, avenues, streets, sidewalks of urban scenario modeled and characterized as a replica of Plaza de Góngora (42°47'52.72" N, 1°38'21.14" W) located in Pamplona, Spain. The area encompasses 380,000 m³ (190 m × 100 m × 20 m) of scenario, and includes: 1 park, 2 motorway avenues, 3 secondary streets, 5 buildings (20 m high), 8 park-bench, 8 medium-lampposts (7 m high), 13 high-lampposts (10 m high), 16 pedestrians, 45 cars, 100 trees and many sidewalks; each of them have its own electromagnetic characteristics for the 3D RL algorithm. The analysis was carried out for frequencies at: 868 MHz, 2.4 GHz and 5.9 GHz and the simulation information is distributed in 380,000 cuboids of 1 m × 1 m × 1 m. The height of the transmitter (Tx) and receiver (Rx) antennas was defined at 1.5 m for cars and 9 m for lampposts. The transmitted power was considered at 0 dBm and the power reference level (sensitivity) was considered at -120 dBm.

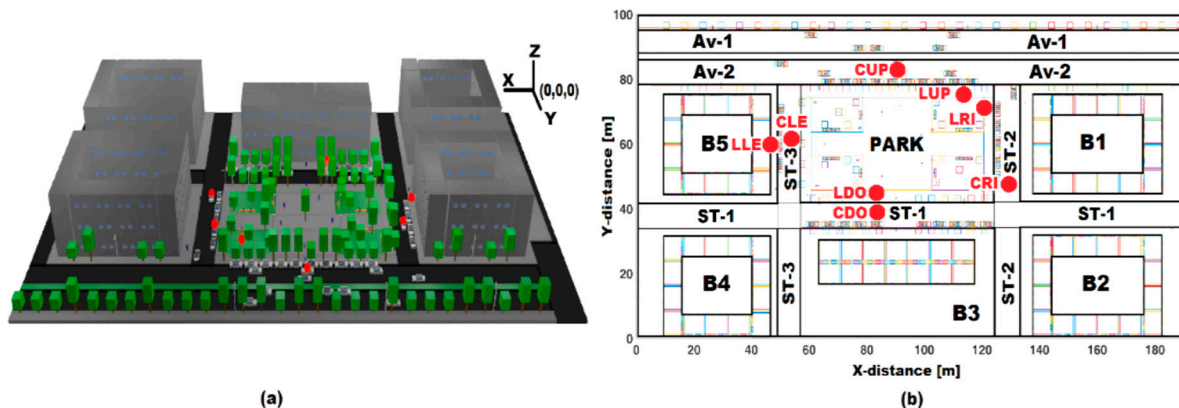


Figure 1. Scenario characterized where (a) is 3D frontal view and (b) is 2D back-view.

Table 1. Identification of different points of interest.

| Description | Abbreviation | Coordinates (x, y, z) [m] |
|--|--------------------|--|
| Main Avenues: L1 L2 | Av-1/Av-2 | (x, 93, 0)/(x, 82, 0) |
| Streets: S1/S2/S3 | ST-1/ST-2/ST-3 | (x, 39, 0)/(54, y, 0)/(130, y,0) |
| Lamppost antennas: Up/Right/Down/Left | LUP/LRI/LDO/LLE | (114, 78, 9)/(126, 73, 9)/(83, 43, 9)/(49, 62, 9) |
| Car antennas: Up/Right/Down/Left | CUP/CRI/CDO/CLE | (91, 82, 1.5)/(130, 50, 1.5)/(84, 38, 1.5)/(54, 62, 1.5) |
| Builds | B1, B2, B3, B4, B5 | Not applicable. |

3. Results

3.1. Received Power

Figure 2 illustrates a surf plot of RP at Z-plane of 1.5 m when: (Figure 2a) the frequency of the transmitter, situated at LUP (Tx-LUP) level (9 m), is 2.4 GHz and (Figure 2b) the frequency of the transmitter, situated at LDO (Tx-LDO) level (9 m), is 5.9 GHz. The 2D map of the scenario located at the base of the Figure 2a,b permits to identify two zones: zone1 (colored), where average RP is above to -120 dBm and where the communication V2I is feasible and, the zone2 (uncolored) where average RP is below to -120 dBm, which does not have especial interest for V2I analysis in the present work.

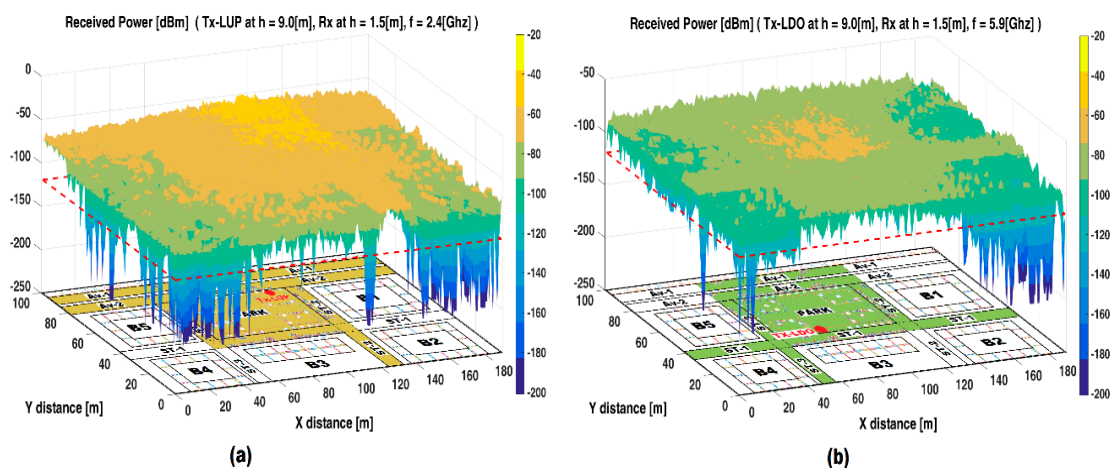


Figure 2. Received Power [dBm] at Z-plane of 1.5 m when: (a) the frequency of Tx-LUP is 2.4 GHz and (b) the frequency of Tx-LDO is 5.9 GHz.

The zone1 of Figure 2a where the RP is above -80 dBm encompass: Av-1, Av-2, ST-1 and ST-2 around the park, the park and ST-2, and, the zone1 of Figure 2b where the RP is above to -100 dBm encompass: part of Av-1 and Av-2, ST-2 and ST-3 around the park, the park and ST-1. From Figure 2, it is important to observe the notorious impact of the link frequency, the distance (from the transmitter), and the density of obstacles (different material properties) have on the propagation phenomenon. The received power level at 2.4 GHz is above than 5.9 GHz (approximately 20 dBm), and we can infer, that received power level at 868 MHz will be above than 2.4 and 5.9 GHz. The position of the Tx. has marked importance in the signal propagation along the avenues and streets: Tx-LUP coverage is feasible for ST-2, Av-1 and Av-2, while Tx-LDO coverage is feasible for ST-1 and only a segment of Av-1 and Av-3. The impact in received power is more pronounced at buildings location. One alternative that will permit an adequate V2I link, is to place 2 RSU: the first near at the intersection of Av-2 and ST-2, and the second near at the intersection of ST-1 and ST-3.

3.2. Time Dispersion Parameters

The analysis of PDP has great importance in WSN to design some general guidelines for deployment. For instance, the cyclic prefix (CP) of adaptive algorithms aimed to increase the spectral efficiency is determined by the maximum access delay or by the RMS delay spread of that environment [10]. In the next section we will encompass: PDP, RMS delay spread and CB.

Power Delay Profile

Figure 3 illustrates the power delay profile when the Tx is located at LUP and Rx are located at CRI (see Table 1 for position references) (frequency 5.9 GHz) and CDO (frequencies 868 MHz and 5.9 GHz).

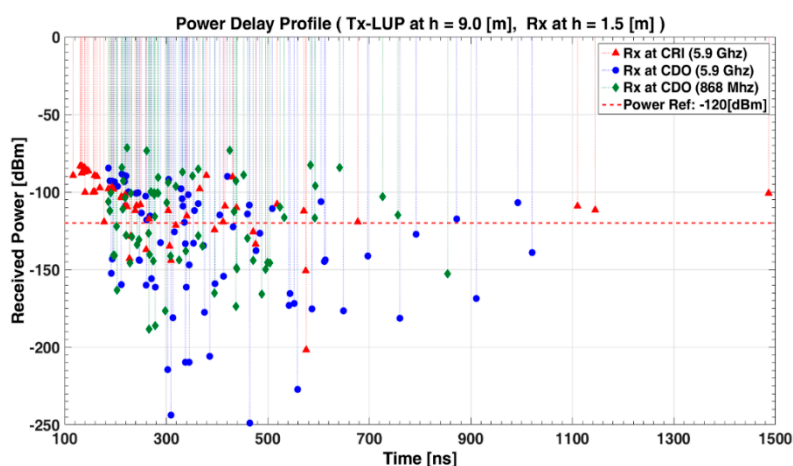


Figure 3. Power delay profile.

Figure 3 shows a large number of power rays (echoes) in the urban scenario in a time span of 100 to 1500 ns, which are highly dependent on the geometrical position relationships among the transmitter, the receiver and the surrounding physical environment. The first ray that arrived at 100 ns corresponds to CRI (14.32 m distance to Tx), located nearest to the Tx than CDO (50.36 m distance to Tx). The time dispersive effects are more notorious for 5.9 GHz (span of 1300 ns approx.) versus 868 MHz (span of 650 ns approx.) when it is compared for CDO. Conversely, the average of RP is less for 5.9 GHz versus 868 MHz for CDO. The density of the received rays is higher in the vicinity of the Tx-LUP due to the multipath propagation. Regarding to delay spread, we can infer it will be lower at distant places of the scenario because the radiation power will be smaller.

3.3. RMS Delay Spread and CB

The RMS delay spread is the square root of the second central moment of the power delay profile and together with the mean excess delay, grossly quantify the time disperse properties of wide band multipath channels, while the CB is a range of frequencies over which two frequencies components have a strong potential for amplitude correlation [11]. The equations used in this work for the calculus of the RMS delay spread and CB, are defined in [11]. The frequency correlation function was considered above 0.9 for the analysis of CB.

Figure 4 shows the phenomena of RMS delay spread and CB for two different Tx locations. The values for RMS delay spread and CB are dependent of the defined sensitivity (−120 dBm) of the WSN simulated and they are necessary to process the received power at each delay. Figure 4a,c show values of RMS delay spread at Tx-LUP and Tx-LDO respectively. The average RMS delay spread for Tx-LUP is 131.48 ns and, 124.90 ns for Tx-LDO. Additional simulations for frequency at 2.4 GHz shows that the average RMS delay spread for Tx-LUP is 160.82 ns and, 156.56 ns for Tx-LUP. From Figure 4a,c, it is shown that areas closer to the antenna Tx have the higher RMS delay spread and the reverse occurs for distant areas to the Tx. It is important to highlight the relationship between the RP, the PDP and the RMS delay spread.

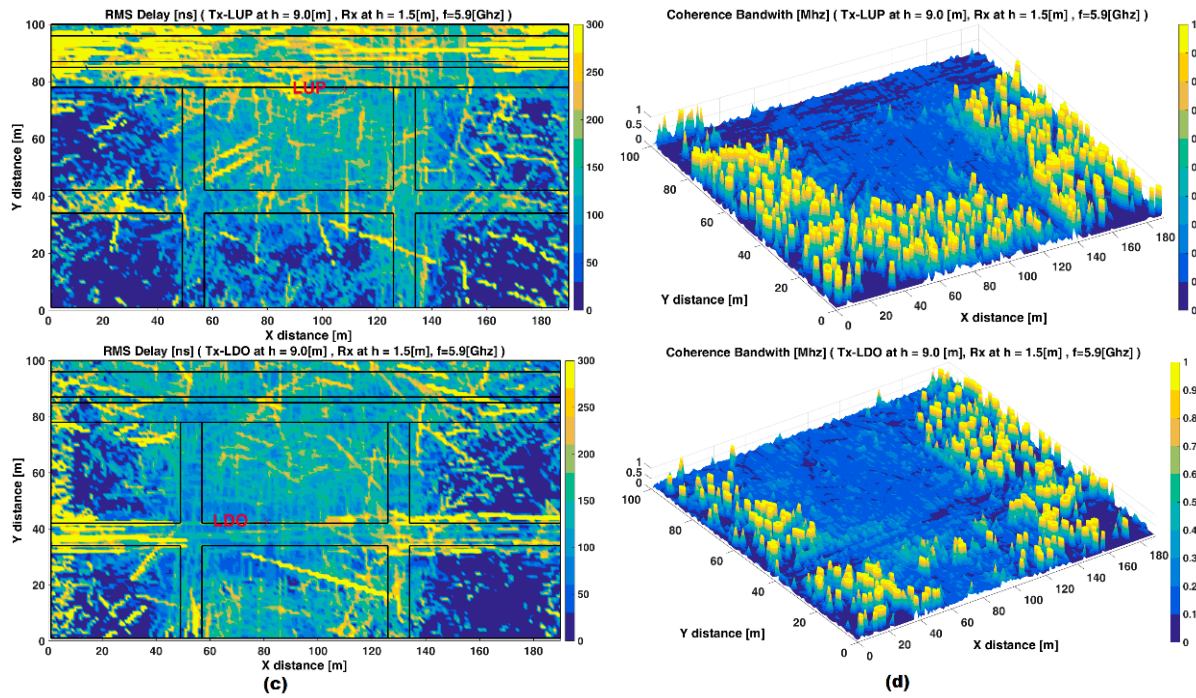


Figure 4. RMS delay spread and CB at Z-plane of 1.5 m for Tx. frequency 5.9 GHz when: (a,b) the transmitter is Tx-LUP, and (c,d) the transmitter is Tx-LDO.

The RP in Figure 2a and the RMS delay spread from Figure 4a exhibit its highest values at zone1 (see Figure 2a): Av-1, Av-2, ST1 and ST-2 around the park, the park, and ST-2. Similar analysis could be done for Figures 2b and 4c. In this way, each spatial sample of the RMS delay spread is associated with a PDP. The Figure 4b,c show the CB at Tx-LUP and Tx-LDO respectively. Given that CB is defined relation derived from RMS delay spread, it is possible to visualize an inverse relationship between CB and RMS delay spread. Indeed, it is important to observe from Figures 2a and 4c an inverse relationship for the received power and CB. With the aforementioned relationships we can affirm that although the highest values of CB displayed at Figure 4b,d correspond to areas with channel availability, however, the RPs values below the sensitivity level, means the wireless communication will be unable.

4. Conclusions and Future Work

Deterministic modelling such as RL are an excellent tool to obtain an adequate estimation of channel propagation parameters in the different parts of the scenario considering all its constituent elements with the aim to deploy an optimal configuration of WSNs in terms of coverage. A 3D in-house ray-launching tool has been used, which enables an accurate evaluation of RP, PDP, RMS delay spread and CB in the context of V2I environments, using WSNs at frequencies of 868 MHz, 2.4 GHz and 5.9 GHz.

In general, factors such as distance from Tx, link frequency, location of RSUs and, obstacles in the LoS will have profound impact in the V2I channel propagation. It is observed lower RP and higher dispersion signal levels at 5.9 GHz. The higher the obstacles in the LoS, the higher the power loss: the buildings yield the more significant power loss, however, they induce the well-known phenomenon of waveguide effect along the streets, which should be taking into account in the deployment of RSUs at intersections. At least 2 RSUs located at specific street intersections are needed to provide optimal V2I wireless communication in terms of coverage.

As a future work, a measurement campaign should be considered for the urban scenery in order to contrast the 3D RL simulation results, with test-field measurements. The identification and characterization of significant areas (i.e., different density of obstacles as buildings, vegetation, etc.) could lead us to the proposal of an empirical or statistical propagation model that account more

environmental variables with the aim of precise results. Geographical area (zone2) with high CB and low RP levels where the V2I communication is unable, could be of special interest in research fields as cognitive radio, V2P, etc.

Acknowledgments: The authors would like to acknowledge the support and collaboration of the Focus Group of Telecommunications and Networks at Tecnológico de Monterrey.

Author Contributions: Fausto Granda, Leyre Azpilicueta and Cesar Vargas-Rosales conducted the simulation and analysis of wireless propagation phenomena and scenario impact. Peio López-Iturri, Erik Aguirre, José Javier Astrain, Jesus Villandagos and Francisco Falcone conceived and prepared the characterization and modelling the urban scenario. Leyre Azpilicueta and Fausto Granda prepared the manuscript.

Conflicts of Interest: The authors declare no conflict of interest. The statements made herein are solely the responsibility of the authors.

References

1. Kochanek, K.D.; Xu, J.; Murphy, S.L.; Minino, A.M.; Kung, H.-C. National Vital Statistics Reports Deaths: Final Data for 2009. *Natl. Cent. Health Stat.* **2012**, *60*, 1–117.
2. Fukushima, M. The latest trend of v2x driver assistance systems in Japan. *Comput. Netw.* **2011**, *55*, 3134–3141.
3. Instituto Nacional de Estadística y Geografía. Accidentes de Tránsito Terrestre en Zonas Urbanas y Suburbanas. Available online: <http://www.inegi.org.mx> (accessed on 5 November 2016).
4. The Institute of Electrical and Electronics Engineers. *IEEE Std 802.11 p-2010. Part 11: Wireless LAN Medium Access Control (MAC) and Physical Layer (PHY). Specifications-Amendment 6: Wireless Access in Vehicular Environments*; IEEE: New York, NY, USA, 2010.
5. Viriyasitavat, W.; Boban, M.; Tsai, H.M.; Vasilakos, A. Vehicular communications: Survey and challenges of channel and propagation models. *IEEE Veh. Technol. Mag.* **2015**, *10*, 55–66.
6. International Telecommunications Union. *P.1411-8 Recommendation. Propagation Data and Prediction Methods for the Planning of Short-Range Outdoor Radiocommunication Systems and Radio Local Area Networks in the Frequency Range 300 MHz to 100 GHz*; P Series: Radiowave Propagation; International Telecommunication Union: Geneva, Switzerland, 2015; p. 49.
7. Matolak, D.W. Modeling the vehicle-to-vehicle propagation channel: A review. *Radio Sci.* **2014**, *49*, 721–736.
8. Azpilicueta, L.; Rawat, M.; Rawat, K.; Ghannouchi, F.; Falcone, F. Convergence analysis in deterministic 3D ray launching radio channel estimation in complex environments. *Appl. Comput. Electromagn. Soc. J.* **2014**, *29*, 256–271.
9. Azpilicueta, L.; Vargas-Rosales, C.; Falcone, F. Deterministic Propagation Prediction in Transportation Systems. *IEEE Veh. Technol. Mag.* **2016**, *11*, 29–37.
10. Hassan, K.; Rahman, T.A. The Mathematical Relationship between Maximum Access Delay and the R.M.S Delay Spread. In Proceedings of the Seventh International Conference on Wireless and Mobile Communications, Luxembourg, 19–24 June 2011; pp. 18–23.
11. Rappaport, T. *Wireless Communications: Principles and Practice*, 2nd ed.; Prentice Hall, Ed.; Communications Engineering and Emerging Technologies Series; Prentice Hall PTR: Upper Saddle River, NJ, USA, 2002.



© 2016 by the authors. Licensee MDPI, Basel, Switzerland. This article is an open access article distributed under the terms and conditions of the Creative Commons Attribution (CC BY) license (<http://creativecommons.org/licenses/by/4.0/>).